

A chlorinated copolymer donor demonstrates a 18.13% power conversion efficiency

Jianqiang Qin^{1, 2}, Lixiu Zhang¹, Chuantian Zuo¹, Zuo Xiao^{1, †}, Yongbo Yuan³, Shangfeng Yang⁴, Feng Hao⁵, Ming Cheng⁶, Kuan Sun^{2, †}, Qinye Bao^{7, †}, Zhengyang Bin^{8, †}, Zhiwen Jin⁹, and Liming Ding^{1, †}

¹Center for Excellence in Nanoscience (CAS), Key Laboratory of Nanosystem and Hierarchical Fabrication (CAS), National Center for Nanoscience and Technology, Beijing 100190, China

²Key Laboratory of Low-grade Energy Utilization Technologies and Systems (MOE), School of Energy and Power Engineering, Chongqing University, Chongqing 400044, China

³Hunan Key Laboratory of Super Microstructure and Ultrafast Process, School of Physics and Electronics, Central South University, Changsha 410083, China

⁴Department of Materials Science and Engineering, University of Science and Technology of China, Hefei 230026, China

⁵School of Materials and Energy, University of Electronic Science and Technology of China, Chengdu 611731, China

⁶Institute for Energy Research, Jiangsu University, Zhenjiang 212013, China

⁷Key Laboratory of Polar Materials and Devices (MoE), School of Physics and Electronic Science, East China Normal University, Shanghai 200241, China

⁸College of Chemistry, Sichuan University, Chengdu 610064, China

⁹School of Physical Science and Technology, Lanzhou University, Lanzhou 730000, China

Citation: J Q Qin, L X Zhang, C T Zuo, Z Xiao, Y B Yuan, S F Yang, F Hao, M Cheng, K Sun, Q Y Bao, Z Y Bin, Z W Jin, and L M Ding, A chlorinated copolymer donor demonstrates a 18.13% power conversion efficiency[J]. *J. Semicond.*, 2021, 42(1), 010501. <http://doi.org/10.1088/1674-4926/42/1/010501>

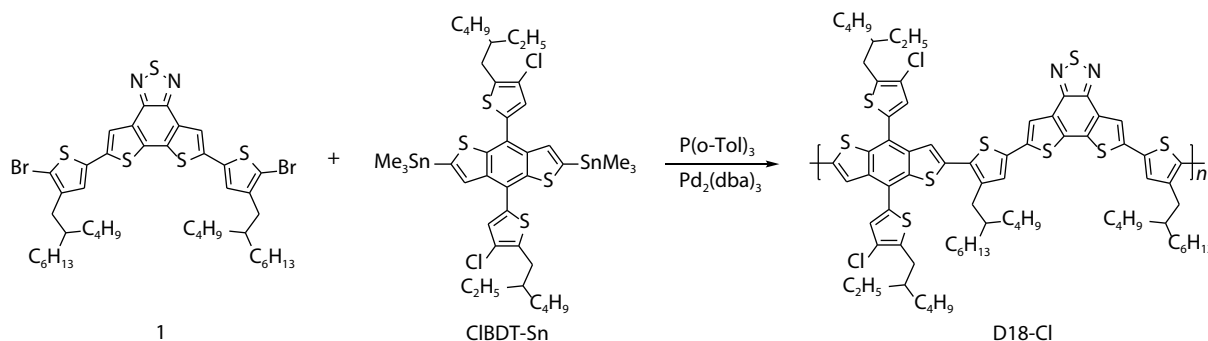
SUPPORTING INFORMATION

1. General characterization

¹H NMR spectrum was measured on a Bruker Avance-400 spectrometer. Absorption spectra were recorded on a Shimadzu UV-1800 spectrophotometer. Cyclic voltammetry was done by using a Shanghai Chenhua CHI620D voltammetric analyzer under argon in an anhydrous acetonitrile solution of tetra-n-butylammonium hexafluorophosphate (0.1 M). A glassy-carbon electrode was used as the working electrode, a platinum-wire was used as the counter electrode, and a Ag/Ag⁺ electrode was used as the reference electrode. D18-Cl was coated onto glassy-carbon electrode and all potentials were corrected against Fc/Fc⁺. AFM was performed on a multimode microscope (Veeco) using tapping mode.

2. Synthesis

All reagents were purchased from J&K Co., Aladdin Co., Innochem Co., Derthon Co., SunaTech Co. and other commercial suppliers. Y6 and N3 were purchased from eFlexPV Co. All reactions dealing with air- or moisture-sensitive compounds were carried out by using standard Schlenk techniques.



Scheme S1. The synthetic route for D18-Cl.

Correspondence to: Z Xiao, xiaoz@nanoctr.cn; K Sun, kuan.sun@cqu.edu.cn; Q Y Bao, qybao@clpm.ecnu.edu.cn; Z Y Bin, binzhengyang@scu.edu.cn; L M Ding, ding@nanoctr.cn

Received 18 DECEMBER 2020.

©2021 Chinese Institute of Electronics

D18-Cl. To a mixture of compound 1^[1] (75.0 mg, 0.083 mmol), ClBDT-Sn (80.5 mg, 0.083 mmol), Pd₂(dba)₃ (2.3 mg, 0.0025 mmol) and P(o-Tol)₃ (7.6 mg, 0.025 mmol) in a Schlenk flask was added toluene (1 mL) under argon. The mixture was heated to reflux for 16 h. Then the solution was cooled to room temperature and added into 150 mL methanol dropwise. The precipitate was collected and further purified via Soxhlet extraction by using CH₂Cl₂ : CHCl₃ (1 : 1), CHCl₃ and chlorobenzene in sequence. The chlorobenzene fraction was concentrated and added into methanol dropwise. The precipitate was collected and dried under vacuum overnight to give D18-Cl as a brown solid (94 mg, 82%). The *M_n* for D18-Cl is 102.7 kDa, with a PDI of 1.95. ¹H NMR (CDCl₃, 400 MHz, δ/ppm): 6.87 (br, aromatic protons), 2.93 (br, aliphatic protons), 0.88-1.53 (br, aliphatic protons).

3. NMR

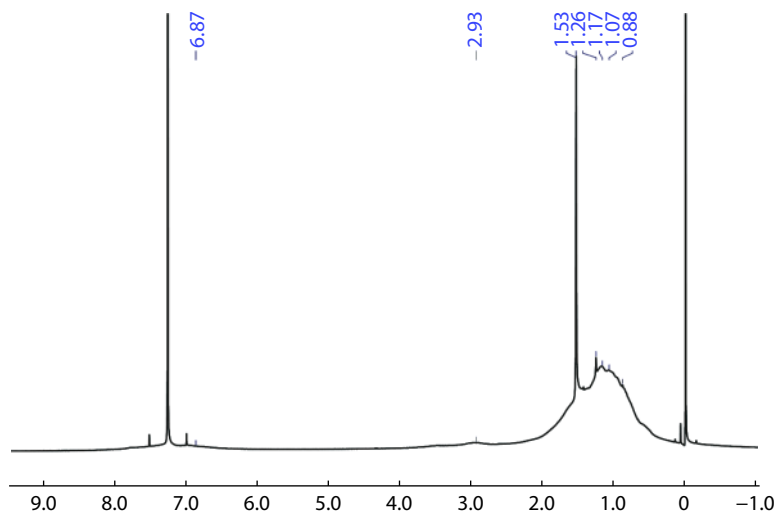


Fig. S1. ¹H NMR spectrum of D18-Cl.

4. CV

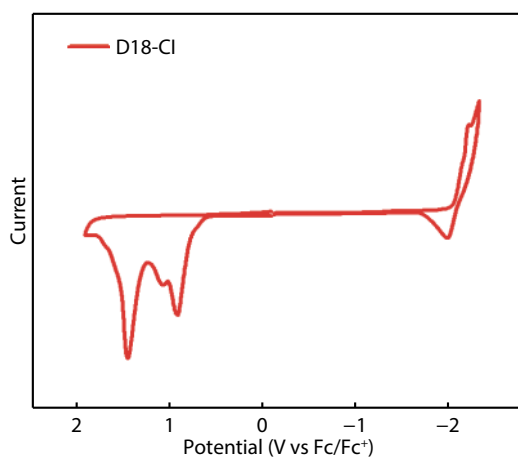


Fig. S2. Cyclic voltammogram for D18-Cl.

5. DFT

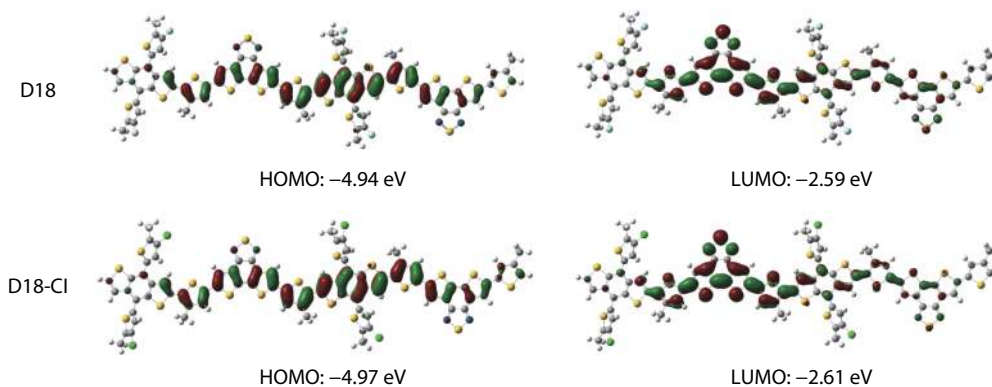


Fig. S3. (Color online) DFT-predicted frontier molecular orbitals and energy levels for D18 and D18-Cl.

6. Device fabrication and measurements

6.1. Conventional solar cells

A 30 nm thick PEDOT:PSS layer was made by spin-coating an aqueous dispersion onto ITO glass (4000 rpm for 30 s). PEDOT:PSS substrates were dried at 150 °C for 10 min. A D18-Cl:acceptor blend in chloroform (CF) was spin-coated onto PEDOT:PSS layer. PDIN (2 mg/mL) in MeOH:AcOH (1000:3) was spin-coated onto active layer (5000 rpm for 30 s). Ag (~80 nm) was evaporated onto PDIN through a shadow mask (pressure ca. 10^{-4} Pa). The effective area for the devices is 4 mm². The thicknesses of the active layers were measured by using a KLA Tencor D-120 profilometer. J - V curves were measured by using a computerized Keithley 2400 SourceMeter and a Xenon-lamp-based solar simulator (Enli Tech, AM 1.5G, 100 mW/cm²). The illumination intensity of solar simulator was determined by using a monocrystalline silicon solar cell (Enli SRC2020, 2 × 2 cm²) calibrated by NIM. The external quantum efficiency (EQE) spectra were measured by using a QE-R3011 measurement system (Enli Tech). The best cells were further tested at NIM for certification. A metal mask with an aperture (2.580 mm²) was used to define the effective area.

6.2. Hole-only devices

The structure for hole-only devices is ITO/PEDOT:PSS/active layer/MoO₃/Al. A 30 nm thick PEDOT:PSS layer was made by spin-coating an aqueous dispersion onto ITO glass (4000 rpm for 30 s). PEDOT:PSS substrates were dried at 150 °C for 10 min. A pure D18-Cl or D18-Cl:acceptor blend in CF was spin-coated onto PEDOT:PSS layer. Finally, MoO₃ (~6 nm) and Al (~100 nm) was successively evaporated onto the active layer through a shadow mask (pressure ca. 10^{-4} Pa). J - V curves were measured by using a computerized Keithley 2400 SourceMeter in the dark.

6.3. Electron-only devices

The structure for electron-only devices is Al/active layer/Ca/Al. Al (~80 nm) was evaporated onto a glass substrate. A D18-Cl:acceptor blend in CF was spin-coated onto Al. Ca (~5 nm) and Al (~100 nm) were successively evaporated onto the active layer through a shadow mask (pressure ca. 10^{-4} Pa). J - V curves were measured by using a computerized Keithley 2400 SourceMeter in the dark.

7. Optimization of device performance

Table S1. Optimization of D/A ratio for D18-Cl:Y6 conventional solar cells^a.

D/A (w/w)	V_{oc} (V)	J_{sc} (mA/cm ²)	FF (%)	PCE (%)
1 : 0.8	0.875	23.97	66.6	13.97 (13.77) ^b
1 : 1.2	0.881	25.85	72.0	16.38 (16.15)
1 : 1.4	0.877	25.89	73.0	16.56 (16.36)
1 : 1.6	0.879	25.79	72.8	16.51 (16.20)
1 : 2	0.881	24.81	72.7	15.90 (15.64)

^aBlend solution: 12 mg/mL in CF; spin-coating: 4000 rpm for 30 s.

^bData in parentheses are averages for 10 cells.

Table S2. Optimization of active layer thickness for D18-Cl:Y6 conventional solar cells^a.

Thickness (nm)	V_{oc} (V)	J_{sc} (mA/cm ²)	FF (%)	PCE (%)
127	0.877	26.12	70.1	16.07 (15.65) ^b
108	0.877	25.89	73.0	16.56 (16.36)
96	0.882	25.42	73.0	16.37 (15.98)
85	0.881	25.11	72.0	15.93 (15.63)

^aD/A ratio: 1:1.4 (w/w); blend solution: 12 mg/mL in CF.

^bData in parentheses are averages for 10 cells.

Table S3. Optimization of DPE content for D18-Cl:Y6 conventional solar cells^a.

DPE (vol%)	V_{oc} (V)	J_{sc} (mA/cm ²)	FF (%)	PCE (%)
0	0.877	25.89	73.0	16.56 (16.36) ^b
0.3	0.865	26.86	73.4	17.07 (16.82)
0.5	0.863	27.08	73.3	17.12 (17.00)
0.7	0.855	27.20	72.7	16.90 (16.63)
1	0.850	27.07	72.9	16.79 (16.59)

^aD/A ratio: 1 : 1.4 (w/w); blend solution: 12 mg/mL in CF; spin-coating: 4000 rpm for 30 s.

^bData in parentheses are averages for 10 cells.

Table S4. Optimization of D/A ratio for D18-Cl:N3 conventional solar cells^a.

D/A (w/w)	V_{oc} (V)	J_{sc} (mA/cm ²)	FF (%)	PCE (%)
1 : 0.8	0.864	25.81	69.8	15.56 (15.14) ^b
1 : 1.2	0.863	26.85	74.3	17.23 (17.15)
1 : 1.4	0.866	26.97	74.6	17.43 (17.23)
1 : 1.6	0.863	27.18	73.8	17.32 (17.18)
1 : 2	0.865	26.47	74.1	16.97 (16.78)

^aBlend solution: 12 mg/mL in CF; spin-coating: 4000 rpm for 30 s.^bData in parentheses are averages for 10 cells.Table S5. Optimization of active layer thickness for D18-Cl:N3 conventional solar cells^a.

Thickness (nm)	V_{oc} (V)	J_{sc} (mA/cm ²)	FF (%)	PCE (%)
125	0.864	26.98	73.9	17.23 (17.04) ^b
112	0.866	26.97	74.6	17.43 (17.23)
101	0.866	26.04	74.5	16.79 (16.56)
88	0.868	25.63	74.3	16.51 (16.23)

^aD/A ratio: 1 : 1.4 (w/w); blend solution: 12 mg/mL in CF.^bData in parentheses are averages for 10 cells.Table S6. Optimization of DPE content for D18-Cl:N3 conventional solar cells^a.

DPE (vol%)	V_{oc} (V)	J_{sc} (mA/cm ²)	FF (%)	PCE (%)
0	0.866	26.97	74.6	17.43 (17.23) ^b
0.3	0.861	27.09	75.6	17.64 (17.38)
0.5	0.859	27.85	75.7	18.13 (17.83)
0.7	0.855	27.47	74.6	17.52 (17.35)
1	0.853	27.27	75.2	17.48 (17.33)

^aD/A ratio: 1 : 1.4 (w/w); blend solution: 12 mg/mL in CF; spin-coating: 4000 rpm for 30 s.^bData in parentheses are averages for 10 cells.

8. NIM certification for D18-Cl:N3 solar cells

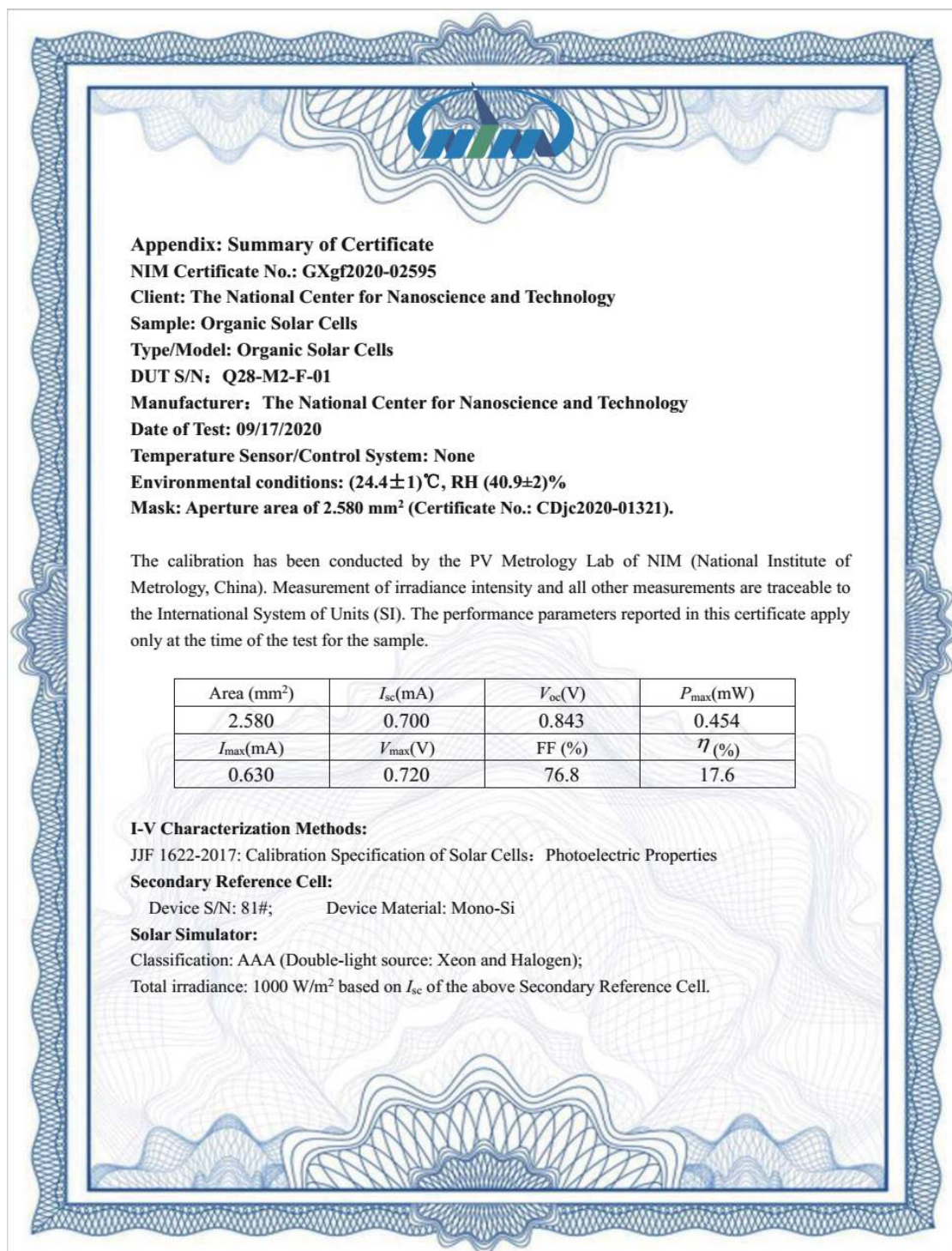


Fig. S4. (Color online) NIM (Beijing) report for D18-Cl:N3 solar cells.

9. Exciton dissociation probability

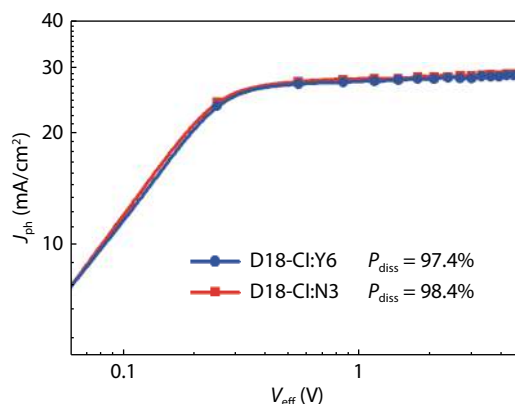


Fig. S5. (Color online) $J_{\text{ph}}-V_{\text{eff}}$ plot.

10. SCLC

Charge carrier mobility was measured by SCLC method. The mobility was determined by fitting the dark current to the model of a single carrier SCLC, which is described by:

$$J = \frac{9}{8} \epsilon_0 \epsilon_r \mu \frac{V^2}{d^3},$$

where J is the current density, μ is the zero-field mobility of holes (μ_h) or electrons (μ_e), ϵ_0 is the permittivity of the vacuum, ϵ_r is the relative permittivity of the material, d is the thickness of the blend film, and V is the effective voltage ($V = V_{\text{appl}} - V_{\text{bi}}$ where V_{appl} is the applied voltage, and V_{bi} is the built-in potential determined by electrode work function difference). Here, $V_{\text{bi}} = 0.1$ V for hole-only devices, $V_{\text{bi}} = 0$ V for electron-only devices^[2]. The mobility was calculated from the slope of $J^{1/2}-V$ plot.

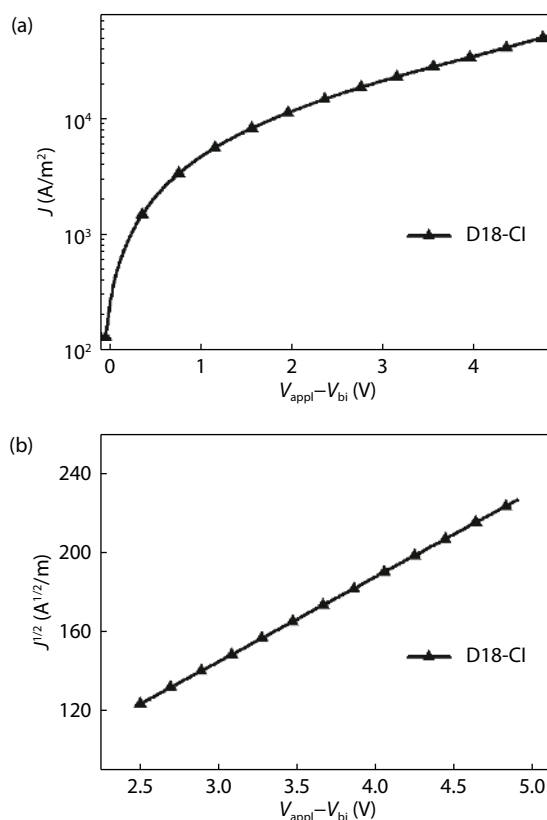


Fig. S6. (a) $J-V$ curve and (b) corresponding $J^{1/2}-V$ plot for the hole-only devices (in dark). The thickness for D18-Cl film is 118 nm.

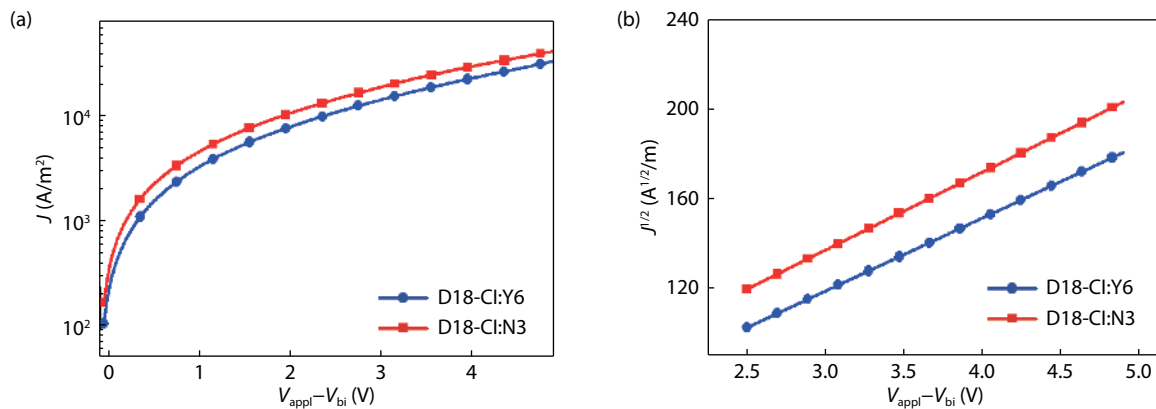


Fig. S7. (Color online) (a) J - V curve and (b) corresponding $J^{1/2}$ - V plot for the hole-only devices (in dark). The thicknesses for D18-Cl:Y6 and D18-Cl:N3 films are 116 and 115 nm, respectively.

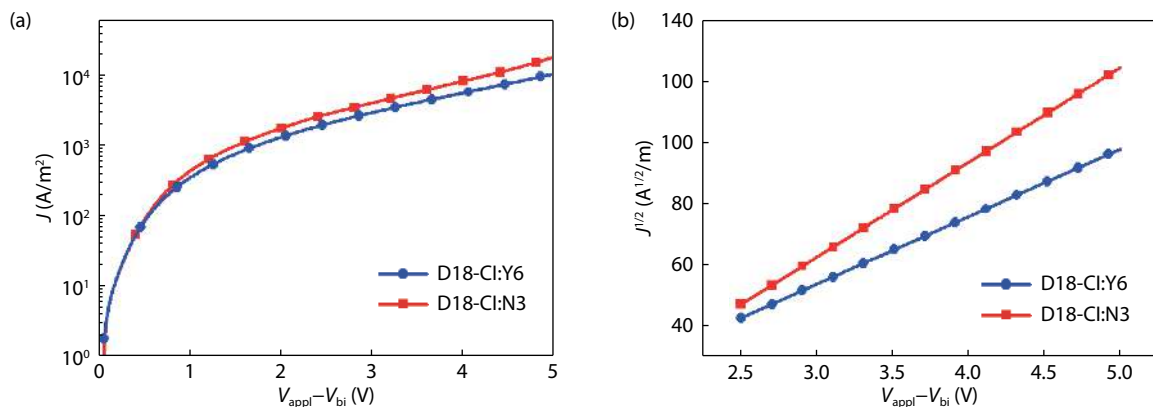


Fig. S8. (Color online) (a) J - V curve and (b) corresponding $J^{1/2}$ - V plot (b) for the electron-only devices (in dark). The thicknesses for D18-Cl:Y6 and D18-Cl:N3 films are 106 and 106 nm, respectively.

Table S7. Hole and electron mobility.

Films	μ_h (cm ² /V·s)	μ_e (cm ² /V·s)	μ_h/μ_e
D18-Cl	1.00×10^{-3}	–	–
D18-Cl:Y6	5.47×10^{-4}	1.94×10^{-4}	2.82
D18-Cl:N3	6.09×10^{-4}	3.83×10^{-4}	1.59

11. Bimolecular recombination

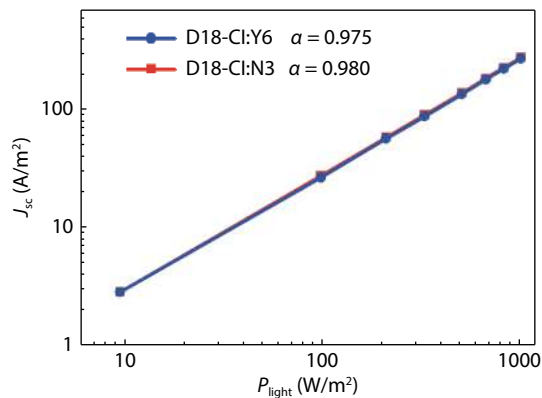


Fig. S9. J_{sc} - P_{light} plot.

12. AFM

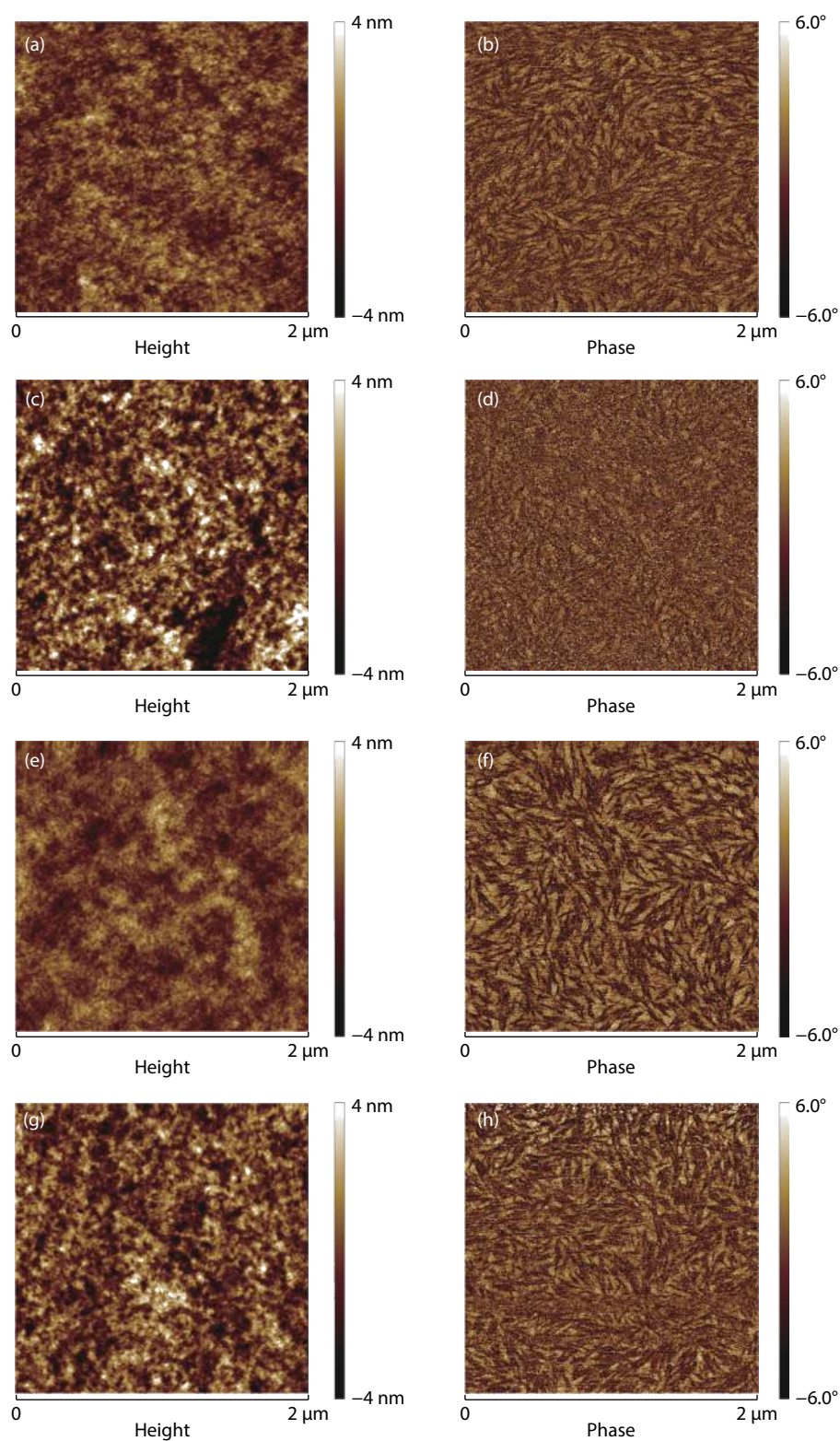


Fig. S10. (Color online) AFM height (left) and phase (right) images for the blend films. (a, b), D18-Cl:Y6 film without additive ($R_{\text{rms}} = 0.82$ nm); (c, d) D18-Cl:Y6 film with 0.5 vol% DPE ($R_{\text{rms}} = 1.52$ nm); (e, f), D18-Cl:N3 film without additive ($R_{\text{rms}} = 0.79$ nm); (g, h) D18-Cl:N3 film with 0.5 vol% DPE ($R_{\text{rms}} = 1.22$ nm). R_{rms} : root-mean-square roughness.

References

- [1] Liu Q, Jiang Y, Jin K, et al. 18% efficiency organic solar cells. *Sci Bull*, 2020, 65, 272
- [2] Duan C, Cai W, Hsu B, et al. Toward green solvent processable photovoltaic materials for polymer solar cells: the role of highly polar pendant groups in charge carrier transport and photovoltaic behavior. *Energy Environ Sci*, 2013, 6, 3022